A Deterministic Least-Squares Approach to Space–Time Adaptive Processing (STAP)

Tapan Kumar Sarkar, *Fellow, IEEE*, Hong Wang, Sheeyun Park, *Member, IEEE*, Raviraj Adve, *Member, IEEE*, Jinwan Koh, Kyungjung Kim, Yuhong Zhang, *Senior Member, IEEE*, Michael C. Wicks, *Fellow, IEEE*, and Russell D. Brown, *Fellow, IEEE*

***Abstract*—A direct data domain (D^3) least-squares space–time adaptive processing (STAP) approach is presented for adaptively enhancing signals in a nonhomogeneous environment. The nonhomogeneous environment may consist of nonstationary clutter and could include blinking jammers. The D^3 approach is applied to data collected by an antenna array utilizing space and in time (Doppler) diversity. Conventional STAP generally utilizes statistical methodologies based on estimating a covariance matrix of the interference using data from secondary range cells. As the results are derived from ensemble averages, one filter (optimum in a probabilistic sense) is obtained for the operational environment, assumed to be wide sense stationary. However, for highly transient and inhomogeneous environments the conventional statistical methodology is difficult to apply. Hence, the D^3 method is presented as it analyzes the data in space and time over each range cell separately. The D^3 method is deterministic in approach. From an operational standpoint, an optimum method could be a combination of these two diverse methodologies. This paper represents several new D^3 approaches. One is based on the computation of a generalized eigenvalue for the signal strength and the others are based on the solution of a set of block Hankel matrix equations. Since the matrix of the system of equations to be solved has a block Hankel structure, the conjugate gradient method and the fast Fourier transform (FFT) can be utilized for efficient solution of the adaptive problem. Illustrative examples presented in this paper use measured data from the multichannel airborne radar measurements (MCARM) database to detect a Sabreliner in the presence of urban, land, and sea clutter. An added advantage for the D^3 method in solving real-life problems is that simultaneously many realizations can be obtained for the same solution for the signal of interest (SOI). The degree of variability amongst the different results can provide a confidence level of the processed results. The D^3 method may also be used for mobile communications.**

***Index Terms*—Atmospheric interference, D^3 approach, object detection, radar clutter, space–time adaptive processing (STAP).**

I. Introduction

FOR airborne radars it is necessary to detect targets in the presence of clutter, jammers, and thermal noise. The airborne radar scenario has been described in [1]–[3] and is summarized here for completeness. This scenario is depicted in Fig. 1. It is necessary to suppress the levels of the undesired interferers well below the weak desired signal. The problem is complicated due to the motion of the platform as the ground clutter received by an airborne radar is spread out in range, spatial angle, and also over Doppler. One way to detect small signals of interest in such a noisy environment is to have a large array providing sufficient power and a large enough aperture to achieve narrow beams. In addition, the array must have extremely low sidelobes simultaneously on transmit and receive. This is very difficult and expensive to achieve in practice. An alternate way to achieve the same goal is through space–time adaptive processing (STAP). STAP is carried out by performing two-dimensional (2-D) filtering on signals that are collected by simultaneously combining signals from the elements of an antenna array (the spatial domain) as well as from the multiple pulses from a coherent radar (the temporal domain). The data collection mechanism is shown in Fig. 2. The temporal domain thus consists of multiple pulse-repetition periods of a coherent processing interval (CPI). By performing simultaneous multidimensional filtering in space and time the goal is not only to eliminate clutter that arrives at the same spatial angle as the target but also to remove clutter that comes from other spatial angles but has the same Doppler frequency as the target. Hence, STAP provides the necessary mechanism to detect low observables from an airborne radar.

In this paper, we consider a pulsed Doppler radar situated on an airborne platform that is moving at a constant velocity. The radar consists of an antenna array, where each element has its own independent receiver channel. The linear antenna array has N elements uniformly spaced by a distance Δ. The radar transmits a coherent burst of M pulses at a constant pulse-repetition frequency. The pulse-repetition interval is inverse of the pulse-repetition frequency. A pulsed waveform of a finite duration (and approximately finite bandwidth) is transmitted. On receive, matched filtering is done where the receiver bandwidth is equal to the transmit bandwidth. Matched filtering is carried out separately on each pulse return after which the signals are digitized and stored. So for each pulse-repetition interval, R time samples are collected to cover the desired range interval. Hence, we term R as the number of range cells. Therefore with M pulses and N antenna elements, each having its own independent receiver channel, the received data for a coherent processing interval consists of RMN complex base-band samples. These samples are often referred to as the data cube consisting of $R \times M \times N$ complex baseband samples of the re-

Manuscript received April 9, 1999; revised April 3, 2000. This work was supported by DARPA and the U.S. Air Force Research Laboratory under Grant F30602-95-1-0014 and N66001-99-1-8922. The work of S. Park was supported by the U.S. Air Force of Scientific Research under Grant F49620-94-1-0421 through the AASERT program.

T. K. Sarkar, H. Wang, S. Park, R. Adve, J. Koh, K. Kim, and Y. Zhang are with the Department of Electrical Engineering and Computer Science, Syracuse University, Syracuse, NY 13244-1240 USA (e-mail: tksarkar@mailbox.syr.edu).

M. C. Wicks and R. D. Brown are with the Air Force Research Laboratory, Sensors Directorate, Rome, NY 13441 USA.

Publisher Item Identifier S 0018-926X(01)00548-8.

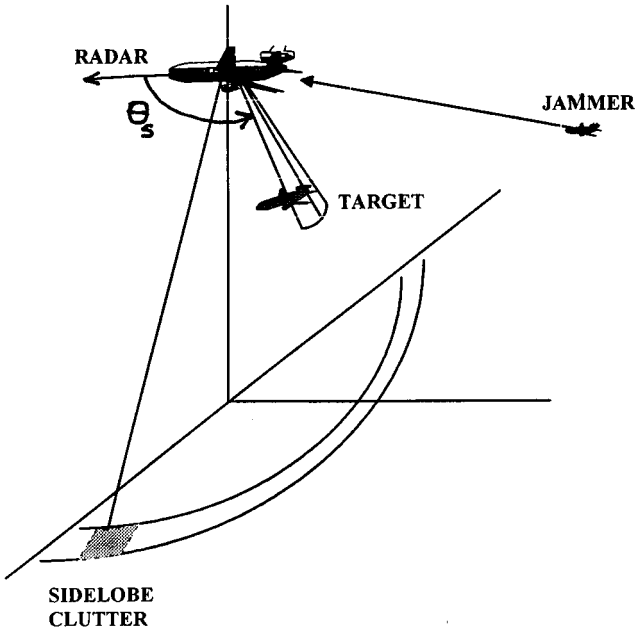

Fig. 1. Scenario of an airborne radar.

ceived pulses. The data cube then represents the voltages defined by $V(m;n;r)$ for $m = 1,\ldots,M; n = 1,\ldots,N$ and $r = 1,\ldots,R$. These measured voltages contain the signal of interest (SOI), jammers, and clutter including thermal noise. A space–time snapshot then is referred to as MN samples for a fixed-range gate value of r.

In the D^3 procedure to be described, the adaptive weights are applied to the single space–time snapshot for the range cell r. Here, a 2-D array of weights numbering N_aN_t is used to extract the SOI for the range cell r. Hence, the weights are defined by $w(p;q;r)$ for $p = 1,\ldots,N_t < M$ and $q = 1,\ldots,N_a < N$ and is used to extract the SOI at the range cell r. Therefore, we essentially perform a high-resolution filtering in two dimensions (space and time) for each range cell.

Conventional STAP processing as available in the published literature deals with the statistical treatment of clutter and this involves estimating a covariance matrix of the interference using data over the range cells [4]–[10]. The statistical procedures thus require secondary data for processing and this is in short supply for a nonstationary environment. In addition, the formation of the covariance matrix and the computation of its inverse is not only computationally intensive but also breaks down under highly nonstationary environment particularly when the clutter scenario changes from land to urban to sea clutter and when there are blinking jammers and hot clutter.

Conventional STAP algorithms develop the necessary equations for the filter weights by first deriving the principle of orthogonality (in the ensemble sense) for wide-sense stationary discrete-time stochastic processes, which are then used to derive the corresponding Wiener–Hopf equations in space–time. In the D^3 least-squares approach the principle of orthogonality is based on the given data samples and this is used to derive a system of equations which provides the mathematical basis of the D^3 least-squares problems. For the adaptive problem in

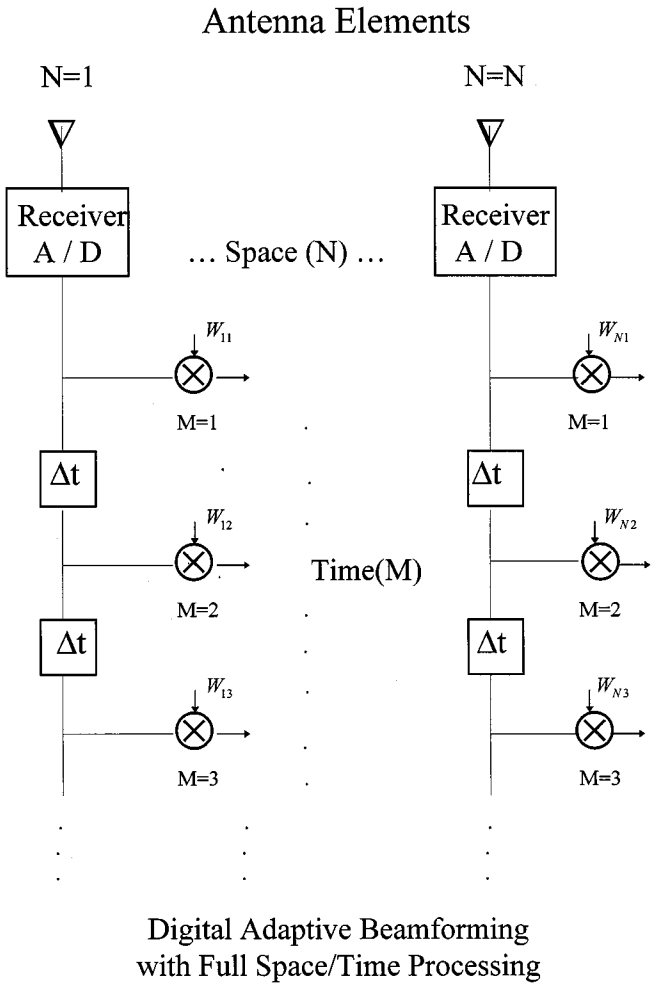

Fig. 2. Data consisting of antenna elements, time sample, and information for each range cell.

one dimension, the methodology has been described in [13], [16] using time averages. This methodology was modified to the single snapshot case in [11] and [12]. From an operational point of view, an optimal method would be a combination of statistical and least-squares STAP methodologies [9].

In this paper, a direct data domain (D^3) least-squares approach developed earlier for spatial adaptive processing is extended to deal with the STAP scenario. In this alternate approach the space–time (multidimensional) filtering is carried out for each range cell separately and directly and, hence, we process the data dealing with each space–time snapshot individually. No secondary data is required in this methodology. Several new techniques are developed for this scenario, based on the previously developed D^3 techniques [11], [12], [16]. These are the techniques based on the eigenvalue approach, forward method, backward method, and the forward–backward method. The next section describes the mathematical details. The airborne radar and the data collection scenario using MCARM data is described in Section III. Numerical results based on processing of this real experimental data is described in Section IV and its performance is compared with conventional approaches using limited examples using real airborne data. This is followed

(a)

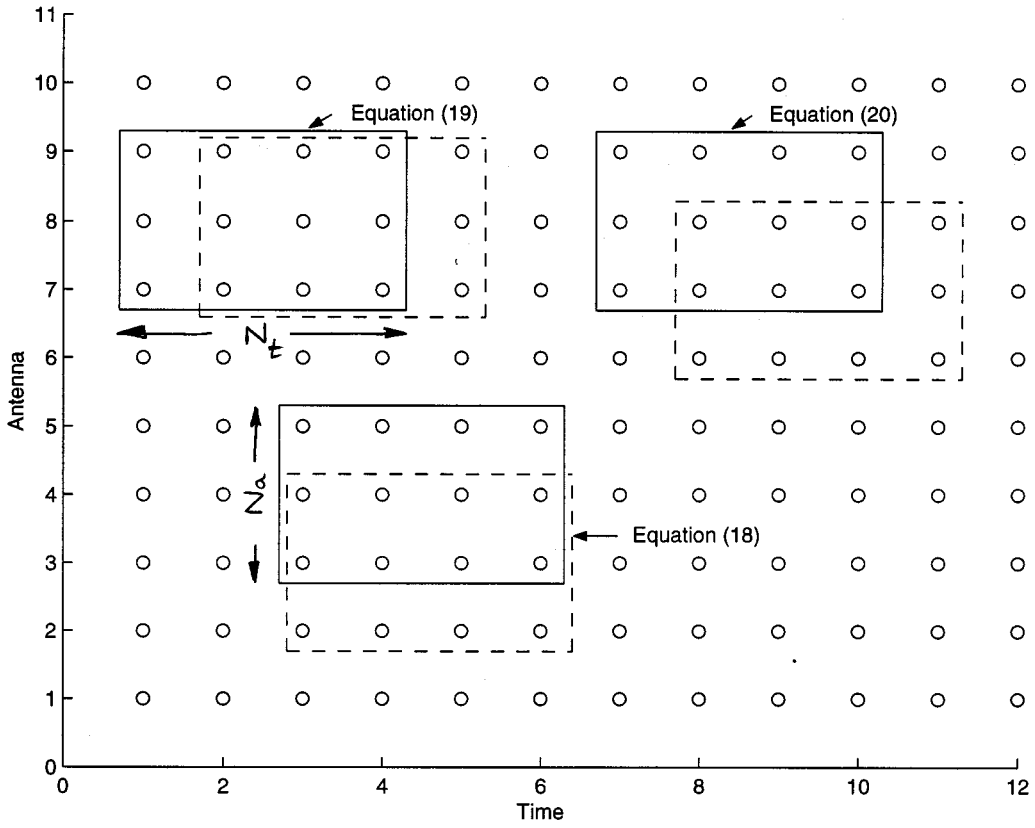

(b)

Fig. 3. (a) Generation of the data cube from space (antenna) and time (Doppler) samples. (b) Explanation of the data processing algorithm.

by some conclusions and a list of references where additional materials can be obtained.

II. Direct-Data Domain (D^3) Least-Squares STAP

A. D^3 Based on the Solution of an Eigenvalue Equation

From the data cube shown in Fig. 3(a), we focus our attention to the range cell r and consider the space–time snapshot for this range cell.

We assume that the SOI for this range cell r is incident on the uniform linear array from an angle θ_s and is at Doppler frequency f_d. θ_s is measured from the nose of the aircraft. Our goal is to estimate its amplitude, given θ_s and f_d only. In a surveillance radar, θ_s and f_d set the look directions and a SOI (target) may or may not be present along this look direction and Doppler. Let us define $S(p;q)$ to be the complex voltage received at the qth antenna element corresponding to the pth time instance for the same range cell r. We further stipulate that the voltage $S(p;q)$ is due to a signal of unity magnitude incident on the array from the azimuth angle θ_s corresponding to Doppler frequency f_d. Hence, the signal-induced voltage under the assumed array geometry and a narrow band signal is a complex sinusoidal given by

$$S_{(p,q)} = \exp\left\{ j \left(\frac{2\pi \Delta q}{\lambda} \cos\theta_s + \frac{2\pi f_d p}{f_r} \right) \right\} \quad \text{for } p = 1, \ldots, M \quad q = 1, \ldots, M \tag{1}$$

where $\lambda =$ wavelength of the RF radar signal $f_r =$ pulse-repetition frequency. Let $X(p;q)$ be the actual measured complex voltages that are in the data cube of Fig. 3(a) for the range cell r. The actual voltages X will contain the signal of interest of amplitude α (α is a complex quantity), jammers, which may be due to coherent multipaths both in the mainlobe and in the sidelobe, and clutter, which is the reflected electromagnetic energy

from the ground. The interference competes with the SOI at the Doppler frequency of interest. There is also a contribution to the measured voltage from receiver thermal noise. Hence, the actual measured voltages $X(p;q)$ are

$$\begin{aligned} X(p,q) &= \alpha \exp\left\{ j\left(\frac{2\pi \Delta q}{\lambda} \cos\theta_s + \frac{2\pi f_d p}{f_r} \right) \right\} \\ &\quad + \text{Clutter} + \text{Jammer} + \text{Thermal noise} \\ &= V(p;q;r). \end{aligned} \tag{2}$$

Now, if one forms the following difference using the signal from range cell r:

$$X(p,q) - \alpha S(p,q) \tag{3}$$

then these elements of the matrix pencil represent the contribution due to the unwanted signal multipaths, jammers, unwanted signals at the same Doppler, and receiver thermal noise. In D[3] adaptive processing, the goal is to take a weighted sum of these matrix elements defined in (3) and extract the SOI, which is going to be α in the range cell r [16].

The total number of degrees of freedom (DOF) then represent the total number of weights and this is the product $N_a N_t$, where N_a is the number of spatial DOF and N_t is the number of temporal DOF. Next, it is illustrated how a direct data domain (D[3]) least-squares approach is taken for the extraction of SOI.

The least-squares procedure for the one-dimensional (1-D) case (i.e., with only the subscript q and no p) is available in [11]–[13], [16]. Here, the same least-squares procedure is extended to two dimensions. Consider the two following matrices C_1 and C_2. The elements of C_1 and C_2 are formed by

$$C_1(x;y) = S(g+h-1;d+e-1) \tag{4}$$

$$C_2(x;y) = X(g+h-1;d+e-1) \tag{5}$$

where

$$1 \le x = g + (d-1)^* N_t \tag{6}$$

$$1 \le y = h + (e-1)N_t \le N_a N_t \tag{7}$$

$$1 \le d \le N - N_a \tag{8}$$

$$1 \le e \le N_a \tag{9}$$

$$1 \le g \le M - N_t \tag{10}$$

$$1 \le h \le N_t \tag{11}$$

so that $1 \le x, y \le N_a N_t$.

Now, if we consider the matrix pencil of size $N_a N_t$

$$[C_2]_{N_a N_t \times N_a N_t} - \alpha [C_1]_{N_a N_t \times N_a N_t} \tag{12}$$

then this represents the contribution of the unwanted signals as the desired components have been canceled out. Please note that the elements of the matrices $[C_2]$ and $[C_1]$ are created out of $X(p,q)$ and $S(p,q)$, respectively, as defined by (4) and (5).

Now in the STAP processing, the elements of the weight vector W are chosen in such a way that the contribution from the jammers, clutter, and thermal noise is zero. Hence, if we define the generalized eigenvalue problem

$$[R][W] = \{[C_2] - \alpha[C_1]\}[W] = 0 \tag{13}$$

then α, the strength of the signal is a generalized eigenvalue and the weights are given by the corresponding generalized eigenvector. Here, W is a column vector of length $N_a N_t$ for the range cell r. Since we have assumed that only the SOI is arriving from θ_s corresponding to the Doppler f_d, the matrix $[C_1]$ is of rank one and hence the generalized eigenvalue equation has only one nonzero eigenvalue which provides the complex value of the signal.

Alternately, one can view the left-hand side of (13) as the total noise signal at the output of the adaptive processor due to jammer, clutter, and thermal noise. One is therefore trying to reduce the noise voltage at the output of the adaptive processor, which is given by

$$N_{\text{out}} = [R][W] = \{[C_2] - \alpha[C_1]\}[W]. \tag{14}$$

The total output noise power then can be obtained as

$$N_{\text{power}} = [W]^H \{[C_2] - \alpha[C_1]\}^H \{[C_2] - \alpha[C_1]\}[W] \tag{15}$$

where H represents the conjugate transpose of a matrix. Our objective is to set the noise power as small as possible by selecting $[W]$ for a fixed signal strength α. This is done by differentiating the real quantity N_{power} with respect to the elements of $[W]$ and setting each component equation to zero. This yields (13).

The total number of DOF $N_a N_t$ is determined by both M and N. Clearly, we need $N_t < M$ and $N_a < N$ so that enough equations can be generated to form (13). Generally, $M \gg N$ and, therefore, there are a larger number of temporal DOF than spatial DOF. The goal, therefore, is to extract the SOI at a given Doppler and angle of arrival in a given range cell r by using a 2-D filter of size $N_a N_t$. The filter is going to operate on the data snapshot depicted in Fig. 3(a) of size NM to extract the SOI.

In real time applications, it is difficult to numerically solve for the generalized eigenvalue problem in sufficient time, particularly if the value $N_a N_t$ representing the total number of weights is large and the matrix $[C_2]$ is highly rank deficient. For this reason, we convert the solution of a eigenvalue problem given by (13) to the solution of a linear matrix equation.

B. Direct Methods Based on the Solution of the Matrix Equation

1) Forward Method: Let

$$z_1 = \exp\left[j \frac{2\pi\Delta}{\lambda} \cos\theta_s \right] \tag{16}$$

$$z_2 = \exp\left[\frac{j 2\pi f_d}{f_r} \right] \tag{17}$$

and we form a reduced rank matrix $[T]$ of dimension $(N_a \times N_t - 1) \times (N_a \times N_t)$ from the elements of the matrix X where

$$\begin{aligned} T(x;y) &= X(g+h-1;d+e-1) \\ &\quad - z_1^{-1} X(g+h-1;d+e) \end{aligned} \tag{18}$$

$$\begin{aligned} T(x+1;y) &= X(g+h-1;d+e-1) \\ &\quad - z_2^{-1} X(g+h;d+e-1) \end{aligned} \tag{19}$$

$$\begin{aligned} T(x+2;y) &= X(g+h-1;d+e-1) \\ &\quad - z_1^{-1} z_2^{-1} X(g+h;d+e) \end{aligned} \tag{20}$$

where

$$1 \le y = N_t(e-1) + h \le N_a N_t \tag{21}$$

for any row x and the variables d, e, g, h take values between the limits defined in (8)–(11). So if we look at the space–time snapshot of Fig. 3(b), we observe how (18)–(20) are implemented. Please note that in (18), the signal-of-interest (SOI) component is canceled from samples taken from different antenna elements at the same time. Similarly (19) represents signal cancellation from samples taken at the same antenna elements at different time instances. Finally, (20) represent signal cancellation from neighboring samples in both space and time. Therefore, we are performing a filtering operation simultaneously using $N_a N_t$ samples of the space–time data as illustrated by Fig. 3(b).

If we consider the three consecutive rows of the matrix T, we observe that they have been formed by taking a weighted difference of a 2-D block of the data of size $N_a N_t$. The weighted difference is taken using the elements of matrix $X(p;q)$. Therefore, $T(x;y)$ is formed by writing the $N_a \times N_t$ difference matrix of (18)–(20) as rows of matrix T. Each of the weighted differences forming $N_a N_t$ elements occupy one row of the matrix T. The three different rows represent three possible choices of the weighted difference between the neighboring elements.

The elements of the matrix T are thus obtained by a weighted subtraction of the induced voltages from the neighboring elements (either in space or in time) so that in these elements the desired signals are canceled out and the elements of T contain no components of the signal corresponding to the Doppler f_d and the direction of arrival θ_s. We choose the weights $[W]$ such that

$$[T][W] = 0 \tag{22}$$

where the column matrix $[W]$ has been generated by arranging the $N_a N_t$ weights from $w(m;n;r)$ in a linear column array corresponding to the processing of the data from range cell r. In order to restore the signal component in the adaptive processing, we fix the gain of the subarray (in both space and time) formed by fixing the first row of the matrix T. The elements of the first row are given by

$$T(1;y) = z_1^{(e-1)} z_2^{(h-1)} \tag{23}$$

where y, e and h are given by (7), (9), and (11), respectively. We set the gain of the system along the direction θ_s of the arrival of the signal and corresponding to the Doppler frequency f_d, at some constant C. Resulting in the matrix equation

$$[T][W] = [Y] = \begin{bmatrix} C \\ \cdots \\ 0 \\ 0 \\ 0 \end{bmatrix}. \tag{24}$$

Once the weight $[W]$ is known by solving (24) the signal strength for the range cell r is estimated from

$$\alpha = \frac{1}{C} \sum_{e=1}^{N_a} \sum_{h=1}^{N_t} W\{N_t(e-1)+h\} X(h;e). \tag{25}$$

Fig. 4. The BAC1-11 carrying the phased array.

The proof of (25) is available in [11].

As noted in [12], (24) can be solved very efficiently by applying the conjugate gradient method along with the fast Fourier transform (FFT). This solution methodology may be implemented in real time as has been demonstrated by its application on a DSP32C signal processing chip [14] for a similar type of problem dealing with Hankel matrices.

It is interesting to note that if the assumed angle of arrival of the signal θ_s and its Doppler f_d is quite different from the actual values, signal cancellation will occur as described in [12] for the adaptive problem. In that case, additional equations are required to constrain the receive 3-dB beamwidth in space and in time following the procedure of [12], [16]. In this paper, this modification has not been considered; as for the examples considered in this paper, it appeared that these factors did not influence our computations.

2) Backward Method: It is well known in the parametric spectral estimation literature that a sampled sequence consisting of a sum of complex exponentials can be estimated by observing it either in the forward direction or in the reverse direction [13, ch. 11]. If we now conjugate the data and form the reverse sequence, then one obtains an equation similar to (24) for the weights. In this case, the first row of the matrix $[T]$ and $[Y]$ are same as before as in (23). The remaining equations of (24), which are given by (18), (19), and (20), now have to be modified. Under the present circumstances, one would obtain the three consecutive rows of the T matrix by taking a weighted difference between the neighboring elements to form

$$\begin{aligned} T(x,y) = {} & X^*(M-h-g+2; N-d-e+2) \\ & - z_1^{-1} X^*(M-h-g+2; N-d-e+1) \end{aligned} \tag{26}$$

$$\begin{aligned} T(x+1;y) = {} & X^*(M-h-g+2; N-d-e+2) \\ & - z_2^{-1} X^*(M-h-g+1; N-d-e+2) \end{aligned} \tag{27}$$

$$\begin{aligned} T(x+2;y) = {} & X^*(M-h-g+2; N-d-e+2) - z_1^{-1} \\ & \cdot z_2^{-1} X^*(M-h-g+1; N-d-e+1) \end{aligned} \tag{28}$$

for any row number x where $*$ represents the complex conjugate of a quantity and h, g, d, and e have been defined in (8)–(11). The row number increases by multiples of three and

$$1 \le y = N_t(e-1) + h \le N_a N_t. \tag{29}$$

Fig. 5. The flight paths of the BAC1-11 and the Sabreliner over the Delmarva Peninsula.

Once the weights are solved for by solving a system of equations similar to (27), the strength of the desired signal at range cell r is estimated from [12], [16]

$$\alpha \approx \frac{1}{C}\sum_{e=1}^{N_a}\sum_{h=1}^{N_t} W\{N_t(e-1)+h\} \times X^*(M-h+1;N-e+1). \quad (30)$$

Thus, the backward procedure provides a second independent realization of the same solution. In a practical environment, where the real solution is unknown, generation of two independent sets of solutions may provide some degree of confidence on the final results.

3) Forward–Backward Procedure: In this procedure, a system of equations are formed by combining the forward and backward solution procedure as described for the 1-D-case [12], [16]. Since, in this process, one is doubling the amount of data available by considering it both in the forward direction and in the reverse direction, one can essentially do one of the following two things. Either increase the number of equations and solve an equation similar to (24) in a least-squares fashion or equivalently increase the number of weights and, hence, the number of DOF by as much as 50%. The second alternative is extremely attractive if one is processing the data on a snapshot-by-snapshot basis due to a highly nonstationary environment. In this way, one can effectively deal with a situation where the number of data samples may be too few to perform any other processing.

Since in this case the total number of data points is $2MN$, the number of degrees of freedom can be increased from the two cases presented earlier. Hence, the number of degrees of freedom in this case will be $N_a'N_t'$, where $N_a' > N_a$ and $N_t' > N_t$. The increase in the number of degrees of freedom depends on the number of antennas N and the time samples M. But clearly $N_a'N_t'$ is significantly greater than N_aN_t. This increase may be by a factor of approximately two when dealing with a data cube where $N = 22$ (the number of antennas in the array) and $M = 128$ (the number of time samples).

III. Description of the Data Collection System

The examples presented in this paper use the data from the MCARM database. A 22 channel $(N = 22)$ phased array containing two rows of 11 subarrays was mounted on the side of a BAC1-11 as shown in Fig. 4. Each subarray combine four elements of a vertically polarized half-wave antennas, which are spaced approximately half a wavelength apart at 1.24 GHz. By assuming that the target is always at 90° in azimuth, all the 22 channels can be processed simultaneously. The beam was pointed downwards in elevation by about 5°. The flight path of the phased array was over the Delmarva peninsula (as defined by the landmass between the Chesapeake Bay and the Atlantic Ocean). In the first experiment, the BAC1-11 received

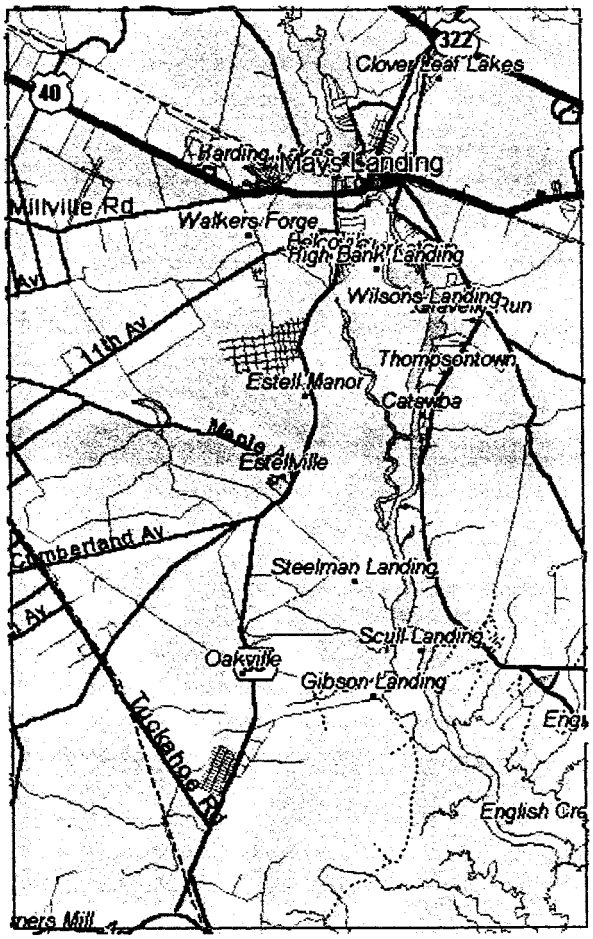

Fig. 6. Scene of the region of ground clutter.

five moving target simulator (MTS) tones from a ground-based transmitter, which was switched on by the transmitted pulse. For the second experiment, the phased array on the BAC1-11 tried to locate a Sabreliner approaching the BAC1-11 in the presence of sea, urban, and land clutter. The data cubes generated from these measurements, which are available from the AF Research Laboratory web site (http://sunrise.deepthought.rl.af.mil), are used to analyze the validity of the algorithms presented in this paper. The details are available in [15]. The geographical region for both flights is shown in Fig. 5 and the regions of ground clutter return in Fig. 6. This indicates that there is possibility of having simultaneously urban, land and sea clutters.

IV. Numerical Example

We next apply the D^3 techniques to the analysis of MCARM data. Specifically, we apply to two specific data sets, namely data set RE050 152.dat and RL050 575.dat. The first one deals with MTS tones in a real clutter environment, whereas the second data set deals with an actual target buried in clutter.

The data was collected by an airborne antenna array. The antenna array had 22 channels in addition to the sum and the difference channel. For each channel, the data in the time domain was sampled at 1984 Hz and there are 128 time samples ($M = 128$).

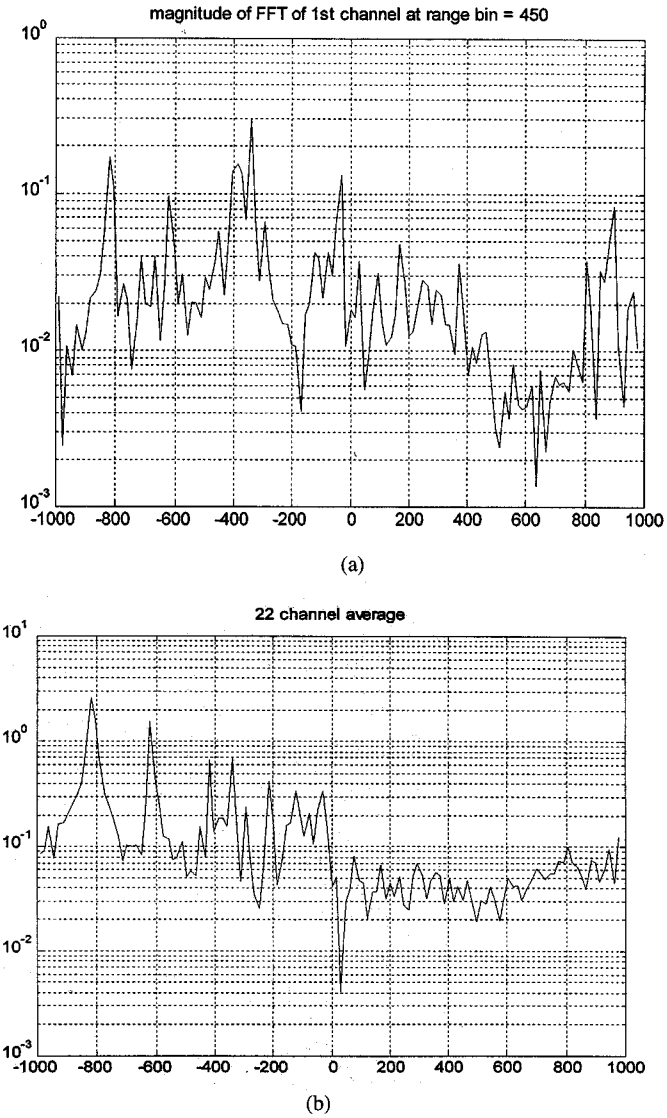

Fig. 7. (a) FFT of a single channel ($\theta_s = 90°$) of the RE050 152.dat. (b) FFT of the sum channel ($\theta_s = 90°$) of the RE050 152.dat.

The third dimension of the data set corresponds to the range profile and there are 630 range bins. The 3 dB beamwidth of the antenna has approximately 7.8°.

For the data cube of the first data set we use RE050 152. In this example, as soon as a ground-based transmitter received part of the transmitted signal from the BAC1-11 it immediately transmitted a set of five moving target simulator (MTS) tones to the BAC1-11. The data consisted of single tones located roughly at 200 Hz apart at Doppler frequencies of -800 Hz, -600 Hz, -400 Hz, -200 Hz, and 0 Hz. The amplitudes of the tones decay roughly by 10 dB so that the amplitude of the -800 Hz is maximum and that at 0 Hz is a minimum. These tones are most dominant in the range bin of $r = 450$. We considered a single channel and the sum of all the 22 channels corresponding to range bin $r = 450$ and performed a 128 point FFT on the time samples. The plot is shown in Fig. 7. The vertical axis plots a normalized decibel plot of the spectrum. The tones at Doppler -800, -600, and -400 are clear. The tones at -200 and 0 Hz are slightly shifted. The FFT spectrum has a resolution

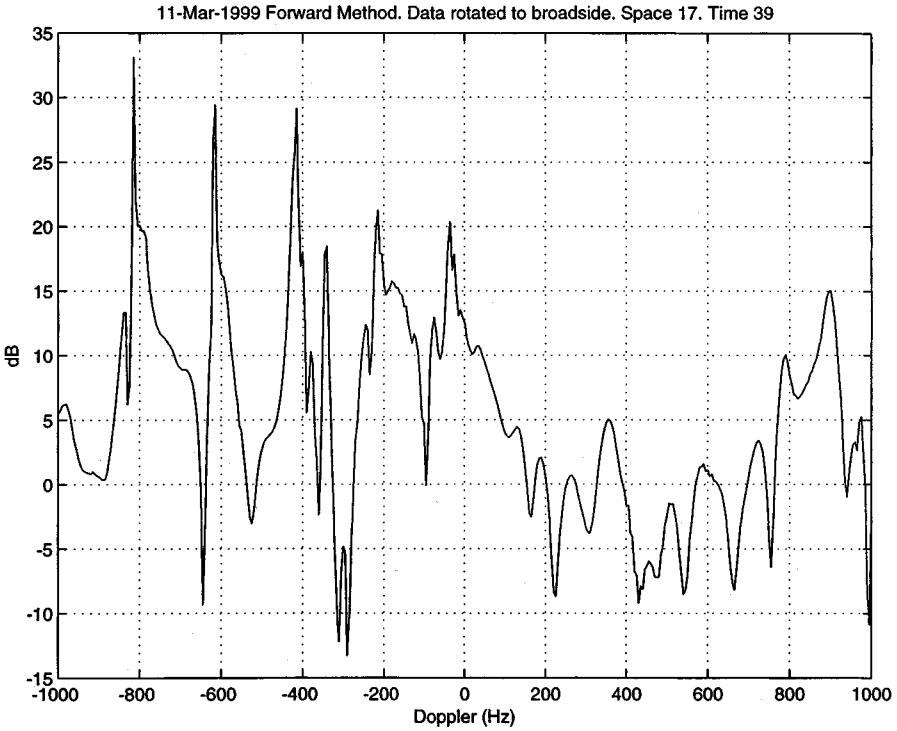

Fig. 8. Utilization of the forward method applied to RE050 152.dat $(S = 17, T = 39)$.

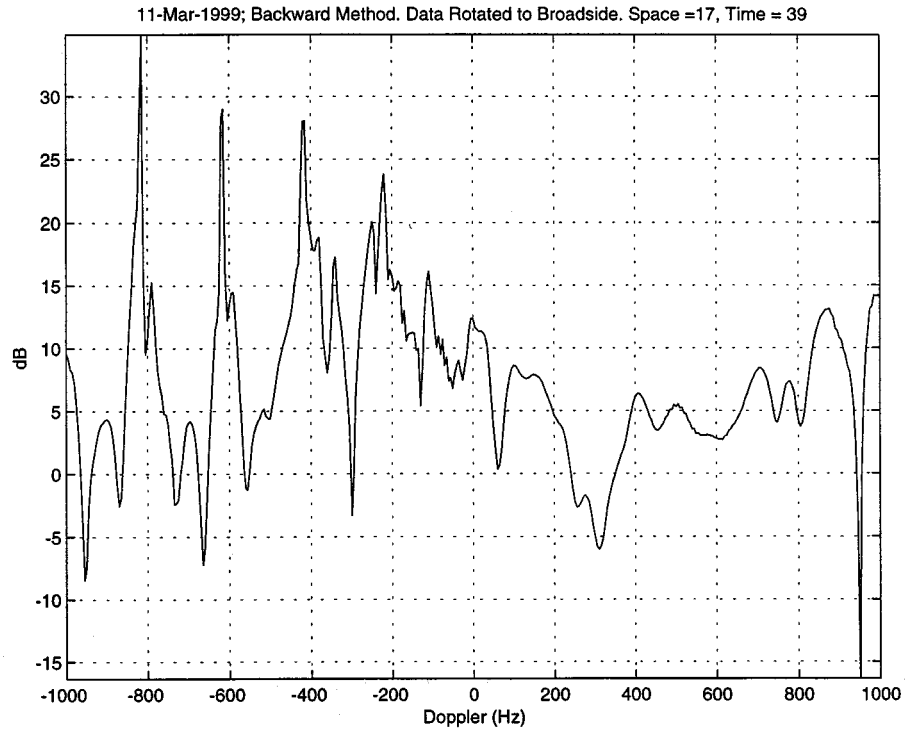

Fig. 9. Utilization of the backward method applied to RE050 152.dat $(S = 17, T = 39)$.

of approximately 15 Hz. Next, we applied the superresolution D^3 analysis where a 2-D filtering technique is applied to each range cell as described by the forward method. The order of the filter required to identify the signals in the presence of clutter consisted of 17 weights or filter taps in space $(N_a = 17)$ and a 39 order filter in time $(N_t = 39)$. So that the total number of degrees of freedom is $N_a N_t$ and is 663. This filter was applied to each range bin, corresponding to the signal of arrival from the

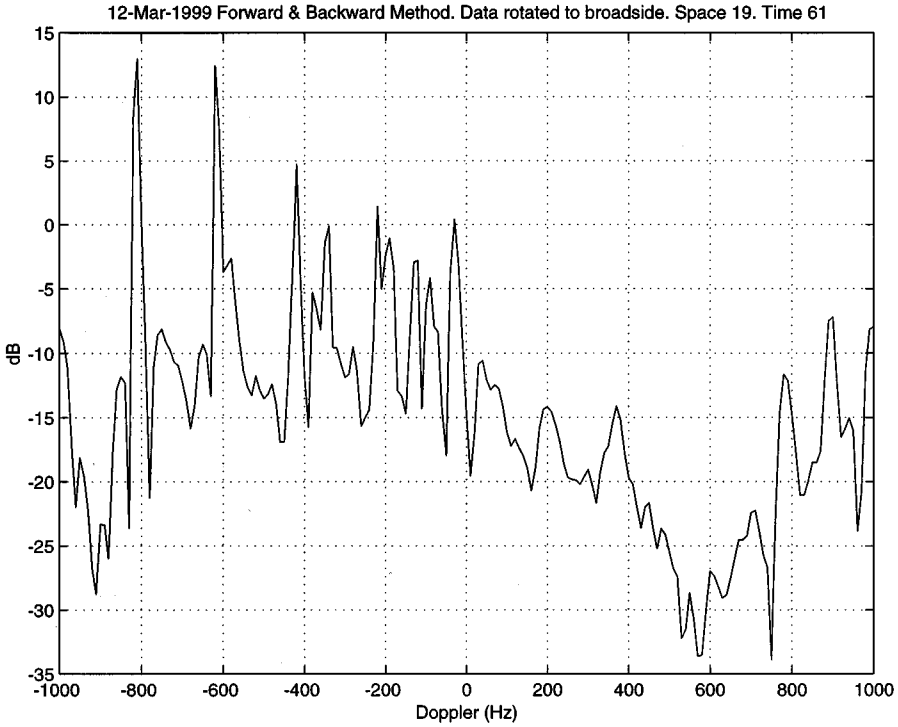

Fig. 10. Utilization of the forward–backward method applied to RE050 152.dat $(S = 19, T = 61)$.

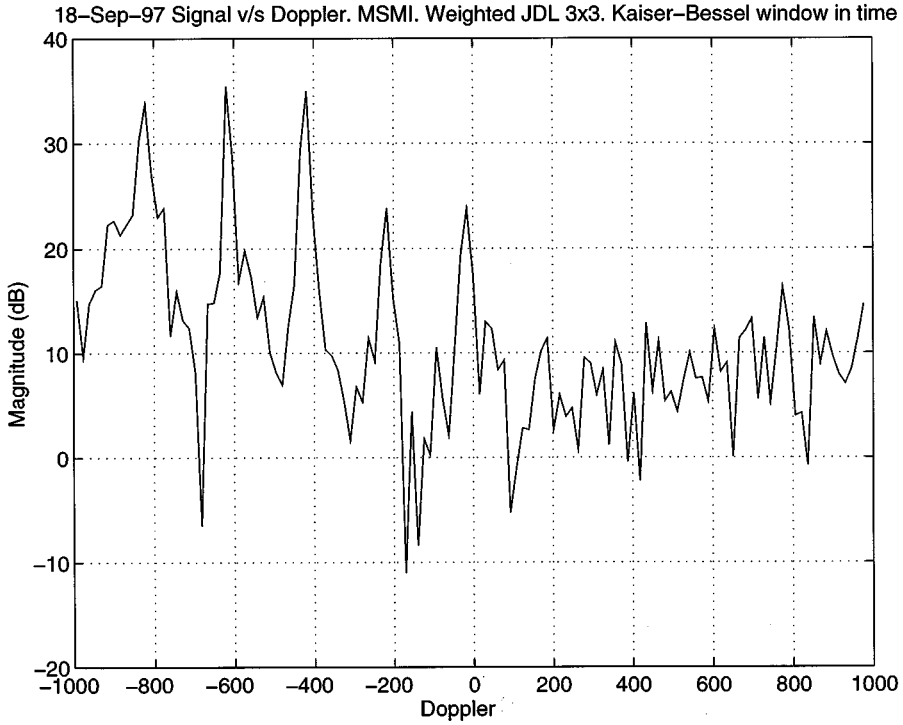

Fig. 11. Utilization of the stochastic method to RE050 152.dat.

broadside direction (i.e., $\theta = 90°$) and the Doppler frequency was swept from -1000 Hz to $+1000$ Hz at intervals of 5 Hz. The estimate of the signal obtained at the output is shown in Fig. 8. In Fig. 9, the estimate of the signal utilizing the backward method is shown using the same order 17×39 space–time filter. Fig. 10 presents the estimate of the signal as a function of Doppler for the forward–backward method. Since, we are using forward–backward method, one has essentially doubled the number of data samples of (22×128) and, for that reason, we use a much higher order filter (19 in space, 61 in time) i.e., $N_a = 19$ and $N_t = 61$. For the forward–backward method the number of degrees of freedom is now 1159. This is nearly

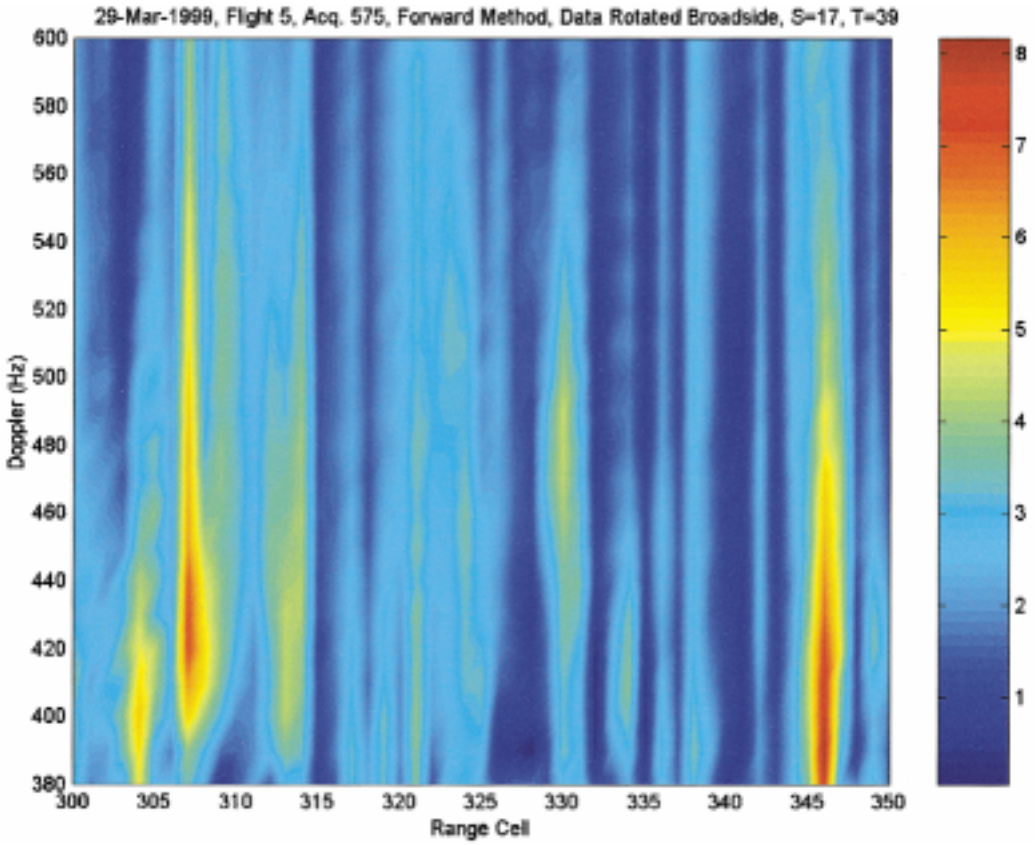

Fig. 12. Application of the forward method to RL050 575.dat.

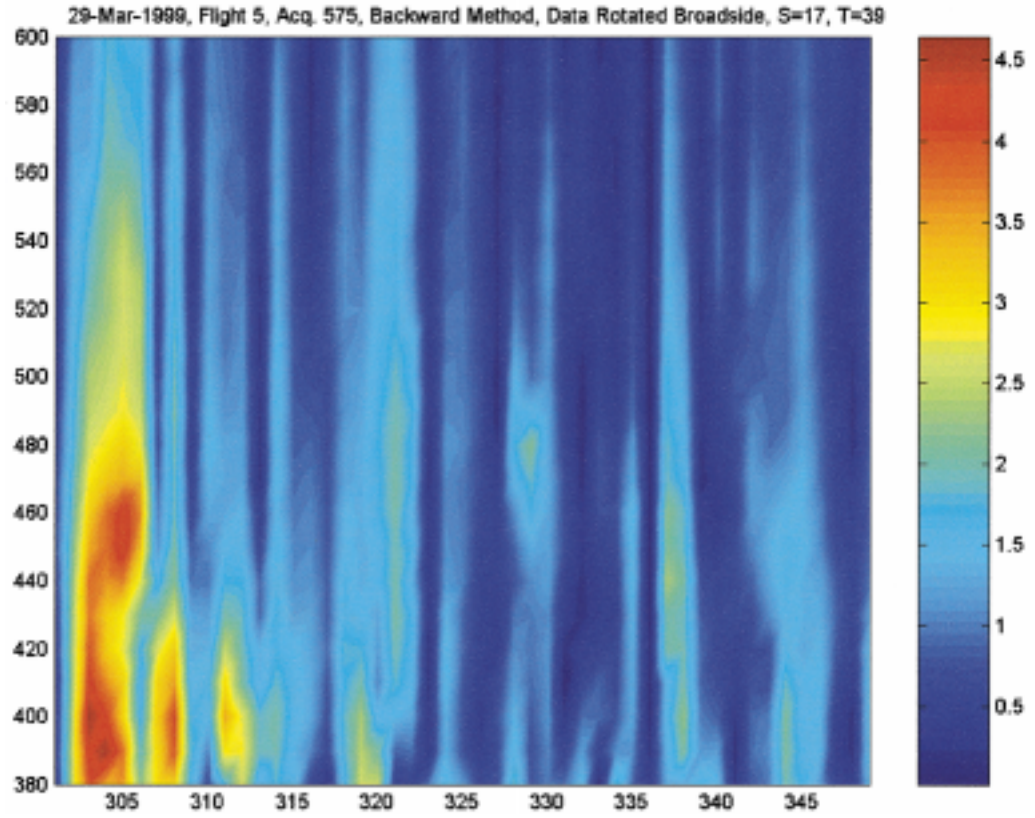

Fig. 13. Application of the backward method to RL050 575.dat.

a twofold increase of the number of degrees of freedom used in either the forward or the backward method. The result is shown in Fig. 10. It is seen that all the three methods provide similar estimates for the tones. However, in some of the methods there

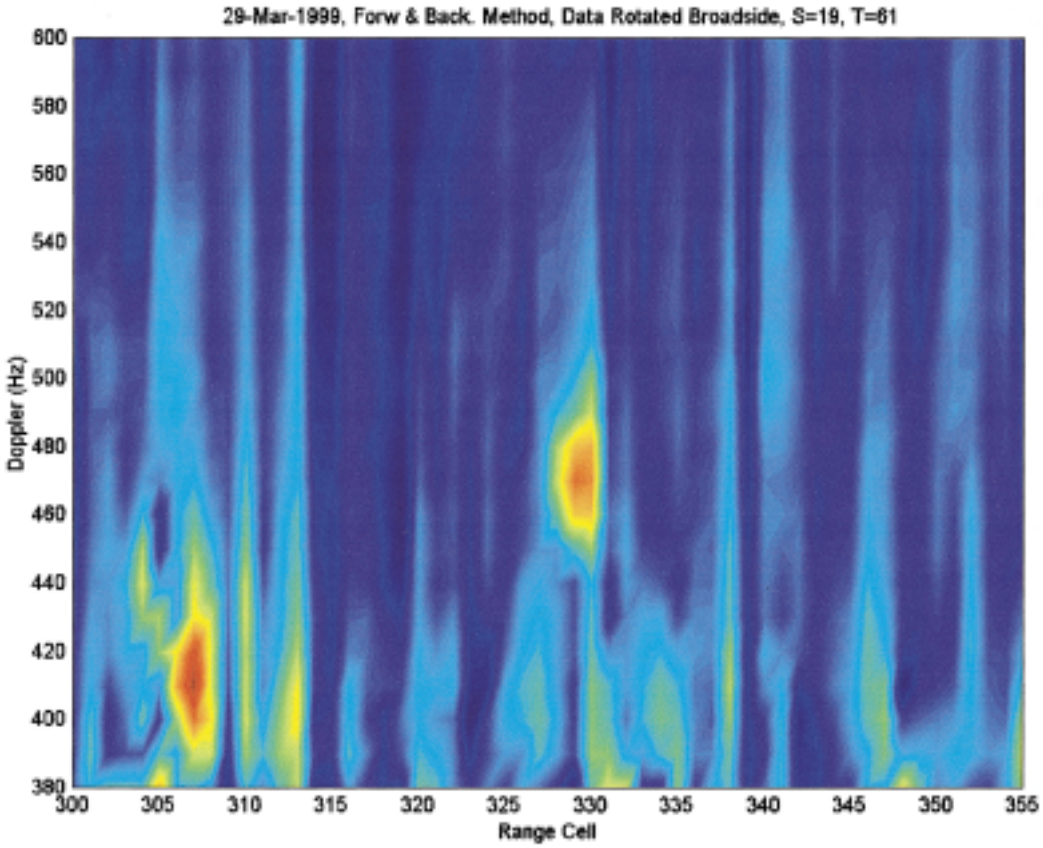

Fig. 14. Application of the forward–backward method to RL050 575.dat.

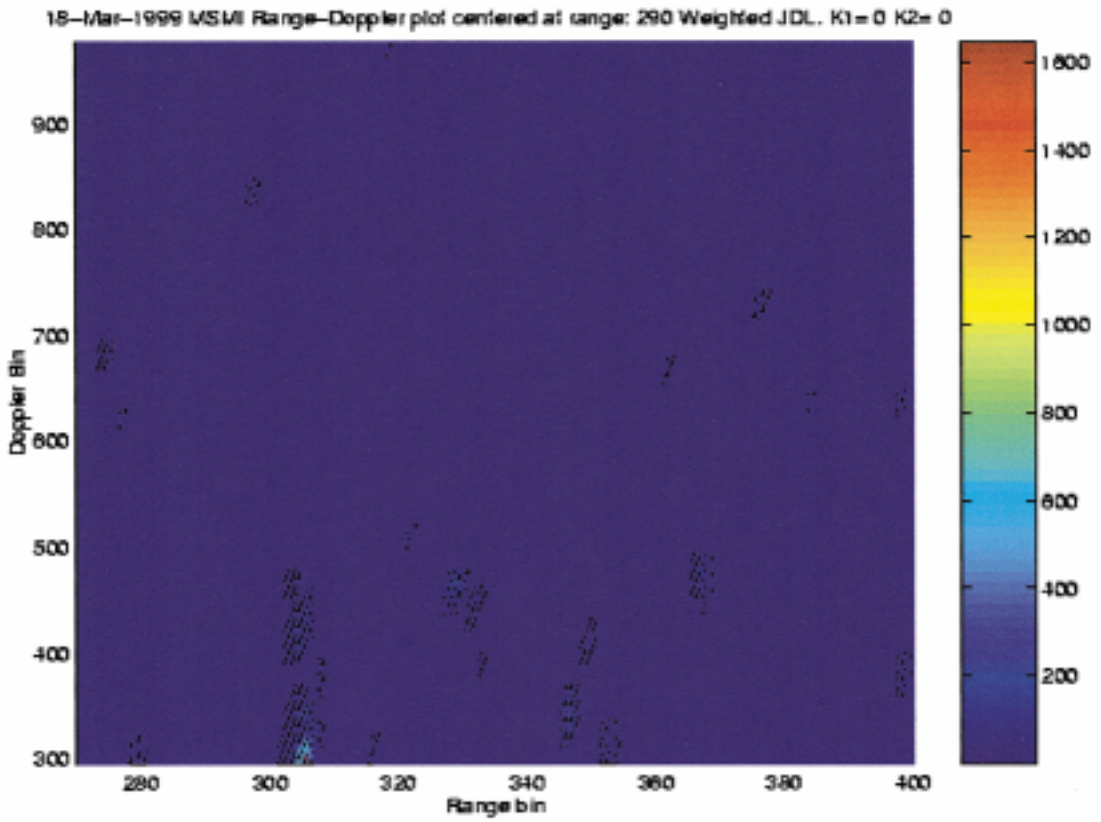

Fig. 15. Application of the stochastic method to RL050 575.dat.

are some spurious peaks. Therefore, simultaneous use of all the three methods would provide a reliable estimate of the signal and will minimize the probability of false alarm. Typical running time for each data point using the forward or the backward

method is less than a minute on a Pentium PC with a clock of 450 MHz. The forward–backward method takes slightly more time than either the forward or the backward method. It is important to note that each range cell/Doppler/look angle can be processed in parallel. Hence, the computational requirements are very modest for real time applications. In all the computations, the value of C in (24) is chosen as unity.

Next, the conventional stochastic method is used to estimate the signal strengths. The application of a 9×9 covariance matrix utilizing a joint domain localized (JDL) stochastic approach [9] is also used to estimate the signals. This is after the data has been Fourier transformed into the Doppler domain utilizing a Kaiser–Bessel window and a 128-point FFT. The result is shown in Fig. 11.

As a second example consider the RL050 575.dat data set. It consists of the data gathered over a flight path over the Delmarva Peninsula. The flight path of the down-looking phased array of the BAC1-11 is shown by the left curve on Fig. 5 on which the particular data set was collected. Its position when it took the data is marked by the circle on the left-hand side. In addition, there is a Sabreliner flying toward the BAC1-11 in a slanted fashion as shown by the second curve of Fig. 5. The position of the Sabreliner is marked on the right-hand side. From the data collected from the geostationary satellites, it appears that the target is at 89° in azimuth and corresponds to the range cell at 318 (this is the second ambiguous range cell, namely $630+318$) and corresponding to the Doppler frequency of approximately $f_d = 520$ Hz. Also, this data set contains received land, sea, and urban clutter from the regions shown in Fig. 6. It also had signal return from highways which may have had some cars traveling by at that time. In the current analysis it is assumed that the signal is coming from $\theta = 90°$, i.e., broadside.

The results of applying the "forward" D^3 least-squares approach using a 17th-order spatial filter and a 39th-order temporal filter is shown in Fig. 12. In this figure, the Doppler values are scanned from 380 to 600 Hz in steps of 10 Hz. The range cells are swept from 300 to 350. Fig. 12 represents the contour plot of the estimated signal return utilizing the forward method with weights of $N_a = 17$ and $N_t = 39$. It is seen that there are some activity around Doppler 500 Hz near the range cells of 308, 330, and 347. Next, the backward method is used to analyze the same data set and using the same number of degrees of freedom $(17 \times 39 = 663)$. The results are shown in Fig. 13. Again large returns around 500 Hz Doppler frequency are observed in the range cells of 305, 320, 330, and 338. The application of the forward–backward method Fig. 14 with the following weights of order $(N_a = 19, N_t = 61)$ results in signal returns which are dominant at range cell of 330. By comparing the results of the three graphs, one could say with confidence which strong signal is a true return corresponding to a particular Doppler and range cell. This is because the three methods are analyzing the same data set in three independent ways and, hence, it makes sense to compare the three results. Fig. 15 provides the response utilizing the stochastic JDL approach of [6]. It is seen there is some weak activity in the range cells of 308 and 330 around the Doppler of 500 Hz. However, without any "ground truth" it is difficult to predict which signal return is actually the saberliner in all of these! This is because there are channel mismatches in the measurements and various uncertainties like the crab angle of the two aircrafts and so on. The actual results show some deviations from the theoretical estimates. There may be several factors of certainties in the measured data like the velocity of each of the aircrafts, their elevation and their direction of travel. However, all the methods predicted returns around the Doppler of 500 Hz in the range bin of 330. This slight discrepancy in Doppler and range can happen due to various factors as outlined. Some shift may occur due to the matched filter processing if the target is not exactly at $\theta_s = 90°$ or due to errors in the array calibration introduced by mutual coupling [17], which were not accounted for in the analysis.

V. Conclusion

A class of direct data domain least-squares adaptive algorithms are presented to estimate the signal in the presence of nonstationary clutter and other possible targets. The problem is solved as an estimation problem rather than as a detection problem as is conventionally done in radar processing. Particularly, the problem of highly nonstationary clutter environment is mitigated by processing the data on a range snapshot by snapshot basis. Unlike the stochastic methods it does not require secondary data cells. This is an advantage, particularly of the direct least-squares data domain approach. Also, these methods are computationally efficient. It is seen from the last four figures that the present approach provides a good contrast in the detection of real targets in nonstationary clutter than the conventional stochastic methods. An added advantage of the D^3 least-squares methodology is that simultaneously at least three independent realizations can be obtained for the same solution. The degree of variability amongst the results between all the three solutions will provide a confidence level for the actual solution, particularly when it is unknown.

References

[1] L. E. Brennan and I. S. Reed, "Theory of adaptive radar," *IEEE Trans. Aerosp. Electron. Syst.*, vol. AES-9, pp. 237–252, Mar. 1973.

[2] L. E. Brennan, J. D. Mallet, and I. S. Reed, "Adaptive arrays in airborne MTI radar," *IEEE Trans. Antennas Propagat.*, vol. AP-24, pp. 605–615, Sept. 1976.

[3] J. Ward, "Space time adaptive processing for airborne radar," Lincoln Lab., , Lexington, MA, Tech. Rep. 1015, Dec. 1994.

[4] R. Klemm, "Adaptive clutter suppression for airborne phased array radars," *Proc. IEEE*, pt. F and H, vol. 130, no. 2, pp. 125–131, Feb. 1983.

[5] E. C. Banle, R. C. Fante, and J. A. Torres, "Some limitations on the effectiveness of airborne adaptive radar," *IEEE Trans. Aerosp. Electron. Syst.*, vol. AES-28, pp. 1015–1032, Oct. 1992.

[6] H. Wang and L. Cai, "On adaptive spatial-temporal processing for airborne surveillance radar systems," *IEEE Trans. Aerosp. Electron. Syst.*, vol. 30, pp. 660–669, July 1994.

[7] J. Ender and R. Klemm, "Airborne MTI via digital filtering," *Proc. IEEE*, pt. F, vol. 136, no. 1, pp. 22–29, Feb. 1989.

[8] F. R. Dickey Jr., M. Labitt, and F. M. Standaher, "Development of airborne moving target radar for long range surveillance," *IEEE Trans. Aerosp. Electron. Syst.*, vol. 27, pp. 959–971, Nov. 1991.

[9] R. S. Adve, T. B. Hale, and M. C. Wicks, "Practical joint domain localised adaptive processing in homogeneous and nonhomogeneous environments: Part 2—Nonhomogeneous environment," *Proc. Inst. Elect. Eng.—Radar, Sonar, Navigat.*, vol. 147, no. 2, pp. 66–74, Apr. 2000.

[10] R. L. Fante, "Cancellation of specular and diffuse jammer multipath using a hybrid adaptive array," *IEEE Trans. Aerosp. Electron. Syst.*, vol. 27, pp. 823–837, Sept. 1991.

[11] T. K. Sarkar and N. Sangruji, "A adaptive nulling system for a narrow-band signal with a look direction constraint utilizing the conjugate gradient method," *IEEE Trans. Antennas Propagat.*, vol. 37, pp. 940–944, July 1989.
[12] T. K. Sarkar, S. Park, J. Koh, and R. A. Schneible, "A deterministic least square approach to adaptive antennas," *Digital Signal Processing— Rev. J.*, vol. 6, pp. 185–194, 1996.
[13] S. Haykin, *Adaptive Filter Theory*, 3rd ed. Englewood Cliffs, NJ: Prentice-Hall, 1996.
[14] R. Brown and T. Sarkar, "Real time deconvolution utilizing the fast Fourier transform and the conjugate gradient method," presented at the *5th ASSP Workshop Spectral Estimation Modeling*, Rochester, NY, 1990.
[15] D. Sloper, D. Fenner, J. Arntz, and E. Fogle, "Multichannel airborne radar measurement (MCARM), MCARM flight test," Rome Lab., New York, NY, vol. I, Tech. Rep. RL-TR-96-49, Apr. 1996.
[16] T. K. Sarkar, J. Koh, R. S. Adve, R. A. Schneible, M. C. Wicks, M. Salazar-Palma, and S. Choi, "A pragmatic approach to adaptive antennas," *IEEE Antennas Propagat. Mag.*, vol. 42, pp. 39–55, Apr. 2000.
[17] R. S. Adve and T. K. Sarkar, "Compensation for the effects of mutual coupling on direct data domain adaptive algorithms," *IEEE Trans. Antennas Propagat.*, vol. 48, pp. 86–94, Jan. 2000.

Tapan Kumar Sarkar (S'69–M'76–SM'81–F'92) received the B.Tech. degree from the Indian Institute of Technology, Kharagpur, India, in 1969, the M.Sc.E. degree from the University of New Brunswick, Fredericton, Canada, in 1971, and the M.S. and Ph.D. degrees from Syracuse University, Syracuse, NY, in 1975.

From 1975 to 1976, he was with the TACO Division, General Instruments Corporation, Sherburne. From 1976 to 1985, he was with the Rochester Institute of Technology, Rochester, NY. He was a Research Fellow at the Gordon McKay Laboratory, Harvard University, Cambridge, MA, from 1977 to 1978. He is currently a Professor in the Department of Electrical and Computer Engineering, Syracuse University, Syracuse, NY. He is on the editorial board of *Journal of Electromagnetic Waves and Applications* and *Microwave and Optical Technology Letters*. He has authored or coauthored more than 210 journal articles and numerous conference papers and has written chapters in 28 books. He is the author of ten books including, *Iterative and Self Adaptive Finite-Elements in Electromagnetic Modeling* (Norwood, MA: Artech House, 1998). His current research interests deal with numerical solutions of operator equations arising in electromagnetics and signal processing with application to system design.

Dr. Sarkar is a registered Professional Engineer in New York State. He received the Best Solution Award in May 1977 at the Rome Air Development Center (RADC) Spectral Estimation Workshop and the Best Paper Award of the IEEE TRANSACTIONS ON ELECTROMAGNETIC COMPATIBILITY in 1979 and at the 1997 National Radar Conference. He received the College of Engineering Research Award in 1996 and the Chancellor's Citation for Excellence in Research, Syracuse University, in 1998. He was an Associate Editor for feature articles of the IEEE Antennas and Propagation Society Newsletter and the Technical Program Chairman for the 1988 IEEE Antennas and Propagation Society International Symposium and URSI Radio Science Meeting. He has been appointed U.S. Research Council Representative to many URSI General Assemblies. He was the Chairman of the Intercommission Working Group of International URSI on Time-Domain Metrology (1990–1996). He is a member of Sigma Xi and the International Union of Radio Science Commissions A and B. He received the title *Docteur Honoris Causa* from Universite Blaise Pascal, Clermont Ferrand, France, in 1998 and the Medal of the City Clermont Ferrand, France, in 2000.

Hong Wang, photograph and biography not available at the time of publication.

Sheeyun Park (S'96–M'98) received the B.S. degree in electrical engineering from the Massachusetts Institute of Technology (MIT), Cambridge, in 1994 and the M.S. and Ph.D. degrees in electrical engineering from Syracuse University, Syracuse, NY, in 1996 and 2000, respectively.

From 1995 to 1998, he was a Research Assistant in the Microwave Laboratory, Syracuse University. From 1998 to 2000, he was a Staff Scientist at Mission Research Corporation, Monterey, CA. He is currently a Software Design Engineer at Agilent Technologies, Santa Clara, CA. His current interests lie in time-frequency analysis, multiresolution harmonic analysis, and spectral analysis of unbounded operators.

Raviraj Adve (S'88–M'96) was born in Bombay, India. He received the B.Tech. degree in electrical engineering from the Indian Institute of Technology (IIT), Bombay, India, in 1990 and the Ph.D. degree from Syracuse University, Syracuse, NY, in 1996.

He is currently with Research Associates for Defense Conversion (RADC) Inc. on Contract with the Air Force Research Laboratory, Rome, NY. He is also an Assistant Professor at University of Toronto, ON, Canada. His research interests include practical adaptive signal processing algorithms with applications in wireless communications and airborne radar systems. He has also investigated the applications of numerical electromagnetics to adaptive signal processing.

Jinhwan Koh was born in Taegu, Korea. He received the B.S. degree in electronics from Inha University, Korea, and the M.S. and Ph.D. degrees in electrical engineering from Syracuse University, Syracuse, NY, in 1997 and 1999, respectively.

He was formerly with Goldstar Electron Semiconductor Company, Korea. He is now a Professor in the Department of Electronics and Electrical Engineering, Kyungpook National University, Taegu, Korea. His current research interests include digital signal processing related to adaptive antenna problems and data restoration.

Kyungjung Kim was born in Seoul, Korea. He received the B.S. degree from Inha University, Korea, and the M.S. degree from Syracuse University, Syracuse, NY. He is currently working toward the Ph.D. degree in the Department of Electrical Engineering at Syracuse University.

He is a Research Assistant at Syracuse University. His current research interests include digital signal processing related to adaptive antenna problems and wavelet transform.

Yuhong Zhang (SM'96), photograph and biography not available at time of publication.

Michael C. Wicks (S'81–M'89–SM'90–F'98) received the undergraduate degrees from Mohawk Valley Community College and Rensselaer Polytechnic Institute, Troy, NY, and the graduate degrees from Syracuse University, Syracuse, NY, all in electrical engineering.

He is a Principal Research Engineer in the U.S. Air Force Research Laboratory in the Sensor Directorate, Radar Signal Processing Branch. He has authored over 125 papers, reports, and patents. His interests include adaptive radar signal processing, wide-band radar technology, ground penetrating radar, radar clutter characterization, and knowledge-based applications to advanced signal processing algorithms, detection, and estimation theory and applied statistics.

Dr. Wicks serves on the board of the SUNY Institute of Technology Foundation, the Mohawk Valley Community College Engineering Science Advisory Council, and the IEEE Aerospace and Electronic Systems Board of Governors and is chairman of the IEEE Radar Systems Panel.

Russell D. Brown (S'72–M'89–SM'91–F'00) was born in Washington, DC, on September 5, 1949. He received the B.S.E.E. and M.S.E.E. degrees from the University of Maryland, College Park, in 1972 and 1973, respectively, and the Ph.D. degree in electrical engineering from Syracuse University, Syracuse, NY, in 1995.

From 1973 to 1978, he served as a Communications Electronics Officer for the U.S. Air Force. Since 1978, he has performed research in radar signal processing at the U.S. Air Force Research Laboratory, Rome, NY.